JMEPEG (2010) 19:428–433
DOI: 10.1007/s11665-009-9504-9

1059-9495/$19.00

Influence of Surface Roughness on Corrosion and Tribological Behavior of CP-Ti After Thermal Oxidation Treatment

E. Arslan, Y. Totik, E. Demirci, and A. Alsaran

(Submitted November 23, 2008; in revised form May 8, 2009)

In this study, tribological and corrosion behavior of commercially pure titanium (CP-Ti) with different surface roughness values after thermal oxidation was investigated. The CP-Ti specimens were prepared with three different roughness values from silicon carbide paper, *Ra* = 0.1, 0.3, and 0.6 μm, and the thermal oxidization process was conducted at a temperature of 850 °C for 8 h in an O_2 atmosphere. Structural, mechanical, corrosion, and tribological properties of untreated and thermally oxidized CP-Ti with different surface roughness values were investigated through x-ray diffraction, scanning electron microscopy, microhardness, potensiostat, and pin-on-disk techniques. The corrosion and tribological behavior of CP-Ti improved as an oxide layer was formed by thermal oxidation. It was observed that the surface roughness had an effect on these characteristics. It was established that the decreased roughness improves the tribological and corrosion properties.

Keywords corrosion, surface roughness, thermal oxidation, wear

1. Introduction

The high strength, low weight ratio, and excellent corrosion resistance inherent to titanium and its alloys have led to a wide and diversified range of successful applications that demand high levels of reliable performance in surgery and medicine as well as in aerospace, automotive, chemical plant, power generation, oil and gas extraction, sports, and other major industries (Ref 1-10). Titanium is available in different grades, unalloyed or alloyed. Unalloyed commercially pure titanium (CP-Ti) is available in four different grades—1, 2, 3, and 4—which are used based on the corrosion resistance, ductility, and strength requirements of the specific application (Ref 11). Grade 2 Ti is typically used for orthopedic applications as well as in aircraft engine parts, marine chemical parts, condenser tubing, and heat exchangers.

The most serious drawback of Ti and its alloys is their poor tribological performance, including a high and unstable friction coefficient, adhesive wear, and sensitivity to fretting wear (Ref 12). There has been a great effort to overcome these disadvantages of titanium and its alloys. Many surface modification processes such as thermal oxidation, physical vapor deposition (PVD), chemical vapor deposition (CVD), plasma nitriding, plasma spraying, and plasma oxidizing have been proposed (Ref 13-16). The Ti surface modified by the relatively simple thermal oxidation technique shows better properties than the others since it produces thick, highly crystalline rutile oxide film (Ref 17). Most of the studies on Ti and its alloys focus on choosing suitable surface modification processes. However, the surface roughness obtained after the surface modification is important in controlling friction, wear, and corrosion behavior. It is well known that the surface roughness is a key parameter affecting the wear and corrosion resistance of components. The characterization of surface topography has become increasingly important in many fields, such as materials, biomedical industry, tribology, and machine condition monitoring (Ref 18).

The rough surfaces decrease both the corrosion and wear resistance because of high ion release rate and plastic deformation under load, respectively (Ref 19, 20). In this study, a thermal oxidation process was chosen to improve the surface properties of CP-Ti. Thermal oxidation treatments were carried out at 850 °C for 8 h because the oxide layer produced at low temperatures and short timings is not thick enough for potential tribological and corrosion applications. The effects of thermal oxidation and surface roughness on the friction, wear, and corrosion behavior of CP-Ti were examined.

E. Arslan, Y. Totik, E. Demirci, and **A. Alsaran**, Surface Technologies and Biomechanics Research Laboratory, Engineering Faculty, Department of Mechanical Engineering, Ataturk University, 25240 Erzurum, Turkey. Contact e-mail: earslan@atauni.edu.tr.

2. Experimental Details

As the substrate material, CP-Ti (Grade 2) with the chemical composition shown in Table 1 was selected. Specimens of 25 mm × 25 mm × 2 mm were prepared by cutting the as-received Ti plate. To evaluate the effect of surface roughness, prior to thermal oxidation, specimens were polished with SiC abrasive papers to *Ra* values of 0.1, 0.3, and 0.6 μm. After polishing, specimens were ultrasonically cleaned in distilled water, followed by acetone. The values of surface roughness before and after thermal oxidation were measured using a Mutitoya Surface Profilometer.

A thermal oxidation temperature of 850 °C was selected for rapid accumulation of oxygen. Thermal oxidation of CP-Ti substrates of different surface roughness values was carried out in a furnace (PLF 120/15). After inserting the substrates into quartz tubes, thermal oxidation was performed by flowing high-purity O_2 into the quartz tubes at 850 °C for 8 h. The substrates were cooled to room temperature in an oxygen-controlled atmosphere after thermal oxidation.

The phase analysis of untreated and thermally oxidized CP-Ti was carried out using x-ray diffraction (XRD; Rigaku D/max-2000 diffractometer) with a CuKα (λ = 1.5404) radiation source. The measurements were carried out for a scan range of 10° to 80° and at a scan speed of 2 °C/min. Interpretation of the x-ray results was undertaken using JCPDS files. Scanning electron microscopy (SEM), using a Jeol 6400, was used to observe the cross sections and the microstructure of thermally oxidized CP-Ti. The microhardness of the specimens was tested using a Buhler Microhardness Tester. For each sample, at least five indentations at different places on the film surface were measured and averaged under a 10 gf load.

The pin-on-disk tribotester (Teer POD2) shown schematically in Fig. 1 was used to determine the tribological properties of the untreated and oxidized specimens. A WC-6%Co ball was used as the counter surface. Pin-on-disk tribotest conditions are given in Fig. 1. After the wear tests, the wear tracks were characterized by SEM.

The electrochemical polarization experiments for investigating the corrosion behavior of untreated and thermally oxidized CP-Ti were carried out using a computer-controlled potentiostat, Potentioscan Wenking PGS 95. Three electrode cell configurations were employed for the polarization measurements. One side of the substrate, whose area is 1 cm^2, was exposed to the solution. The polarization measurements of the specimens were conducted in a 0.5 M NaCl solution. The electrochemical cell consists of untreated and thermally oxidized CP-Ti as the working electrode, a standard Ag/AgCl reference electrode, and a platinum counter electrode. In the potentiodynamic polarization tests, the working electrode was immersed in the test solution and then polarized from the corrosion potential at a scan rate of 1 mV s^{-1} in the anodic and cathodic directions, after an initial potential stabilization of 1 h.

Table 1 The chemical composition of CP-Ti (Grade 2)

Element, wt.%					
Ti	**C**	**Fe**	**H**	**N**	**O**
92.2	0.1	0.3	0.015	0.03	0.25

3. Results and Discussion

Roughness analysis of the surfaces of the untreated and thermally oxidized specimens was conducted using a surface profilometer and SEM. Figure 2 shows the difference in roughness between untreated and thermally oxidized CP-Ti. The surface topographies achieved from the SEM analyses after thermal oxidation are also shown in the figure. The surface roughness values before thermal oxidation, *Ra* = 0.1, 0.3, and 0.6 μm, increased with 8 h of thermal oxidation at 850 °C. The surface roughness values of the substrate were *Ra* = 0.54, 0.64, and 0.7 μm after the thermal oxidation process. The increase in the surface roughness was consistent with the literature (Ref 21-23). In the case of specimens with high substrate surface roughness values, the increase in surface roughness as a result of thermal oxidation was slight as compared to the other specimens. This situation is related to the progress of the oxide layer through the deep valleys to the high peaks, due to the increasing surface area.

Figure 3 shows the cross section of untreated and thermally oxidized CP-Ti. When the cross section of untreated CP-Ti was examined, the passive oxide layer formed naturally was seen on the surface (Fig. 3a). After thermal oxidizing, two zones were identified as indicating inner and outer layers. Figure 3(b) shows a reasonably compact and adherent oxide layer, an oxygen diffusion zone, and the microstructure of thermally oxidized CP-Ti. It is clearly seen from the micrograph in Fig. 3 that the diffusion zone was in a form similar to that of a coral-grown process (Ref 24). In addition, the surface hardness of the oxide layer formed after thermal oxidizing for 8 h at 850 °C was 1097 HV.

Phase analysis of the oxide layer formed after thermal oxidation was carried out by XRD analysis. Figure 4 shows the XRD patterns of thermally oxidized CP-Ti with different surface roughness values. Only the rutile oxide phase was observed in all specimens. As known, rutile is the stable structure of TiO_2, whereas anatase and brookite are metastable structure of TiO_2 (Ref 25). The rutile phase formed on surfaces of Ti and its alloys oxidized at 850 °C was in agreement with the literature (Ref 26-28). In addition, a secondary phase was determined at 2θ = 70°. This phase was defined as the oxygen-diffused Ti(O) situated below the rutile layer (Ref 29, 30). On the other hand, the rutile layer formed at the selected surface roughness values did not show any clear preferred growth orientation.

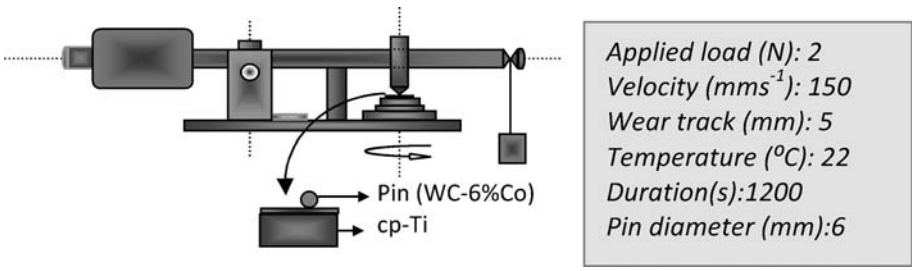

Fig. 1 Pin-on-disk tribotester and test conditions

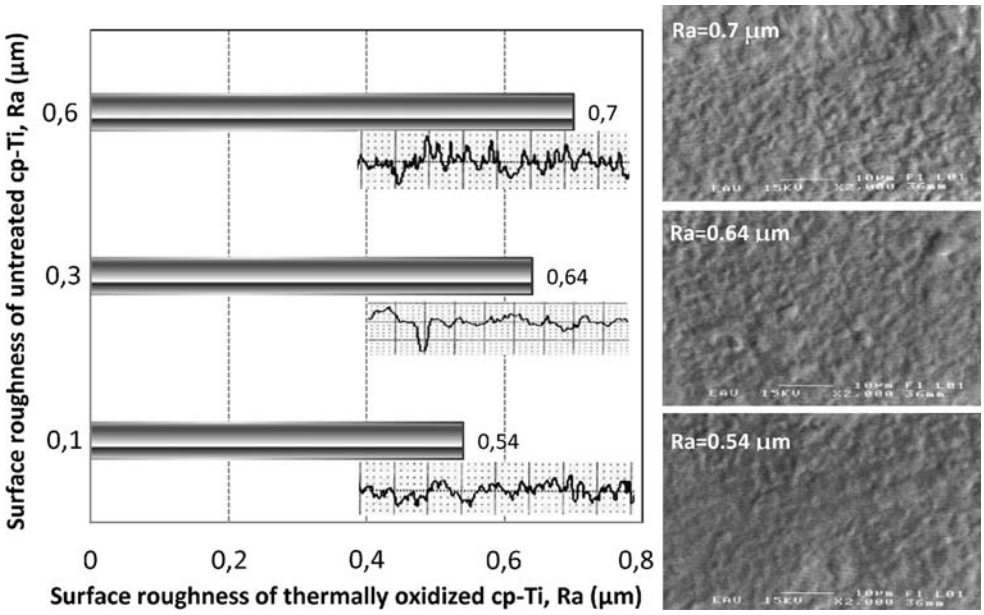

Fig. 2 The roughness values between untreated and thermally oxidized CP-Ti and surface topography of thermally oxidized CP-Ti

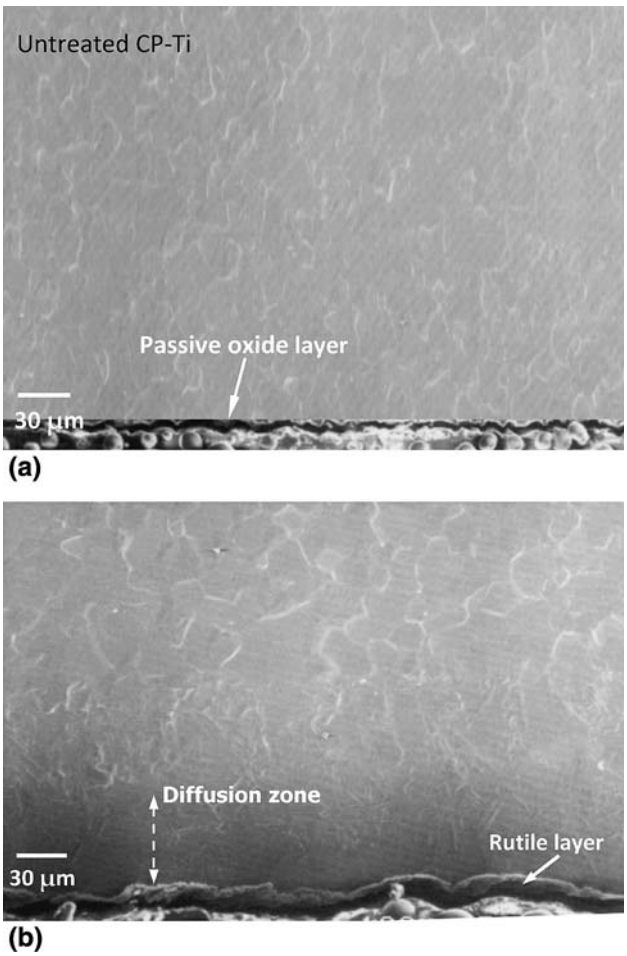

Fig. 3 The cross-sectional image of (a) untreated and (b) thermally oxidized CP-Ti at 850 °C for 8 h

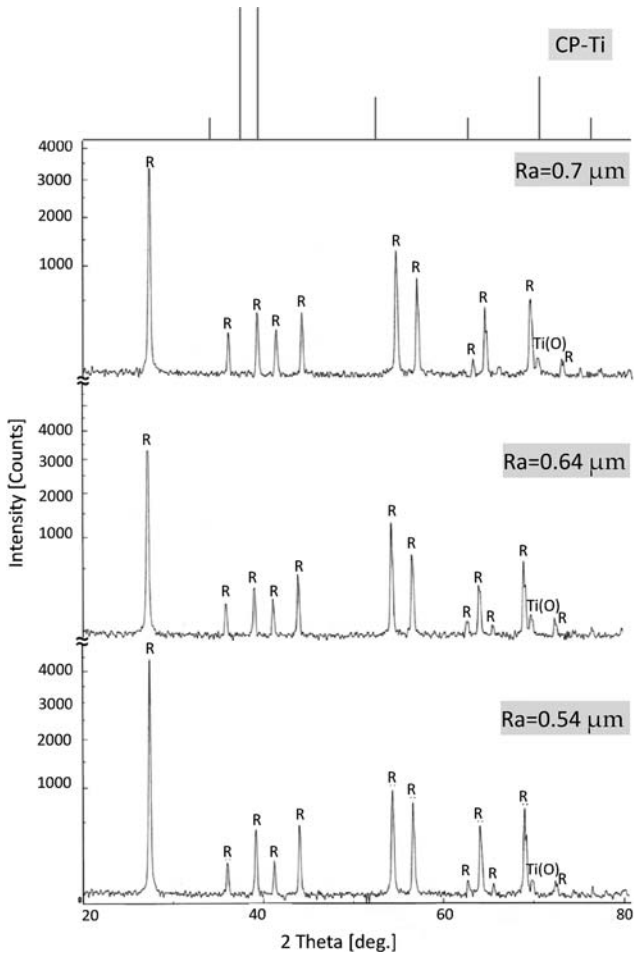

Fig. 4 The XRD patterns of untreated and thermally oxidized CP-Ti with different surface roughness values

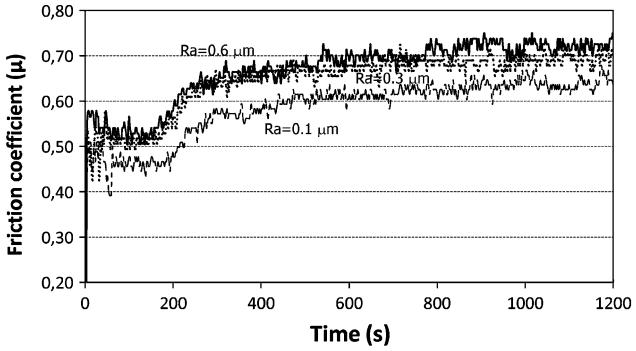

Fig. 5 The friction coefficient curves of untreated CP-Ti

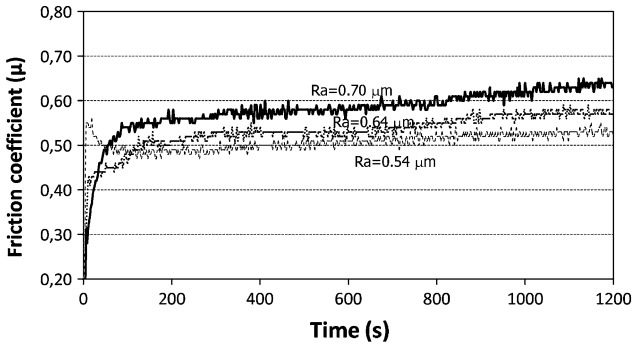

Fig. 6 The friction coefficient curves of thermally oxidized CP-Ti

The tribotests, which were carried out to evaluate the tribological performance of thermally oxidized CP-Ti, showed that the surface topography considerably affected the tribological performance. Figures 5 and 6 show the changes in the friction coefficient curves with respect to time of untreated and thermally oxidized CP-Ti with different surface roughness values, respectively. It is obvious from Fig. 5 and 6 that the surface roughness affected the friction coefficient of both the untreated and oxidized specimens. In each case, the friction coefficient increased with increasing surface roughness. As can be seen in Fig. 5, untreated CP-Ti displayed high and varying friction coefficients. For the specimens with surface roughness values of Ra = 0.1, 0.3, and 0.6, friction coefficients of 0.63, 0.68, and 0.74 were obtained, respectively. On the other hand, thermal oxidation of CP-Ti considerably improved the friction coefficients (Fig. 6). After the oxidation process, the specimens with surface roughness values of Ra = 0.54, 0.64, and 0.7 exhibited friction coefficients of 0.48, 0.53, and 0.58, respectively. Despite the increased roughness values obtained after oxidation, lower friction coefficients were obtained as compared to the untreated specimens. In addition, the friction graphs were smoother and displayed much less fluctuation as compared with that of the untreated CP-Ti. In the literature, the decrease in the friction and wear of the thermally oxidized samples is explained in two ways. First, when two surfaces are in contact with each other, the stress causes the surfaces to deform elastically and plastically. Thermal oxidation limits the plastic and elastic deformation between layers, considerably decreasing the friction and wear. Second, the oxygen deficiency of the rutile phase decreases the friction by causing a low shear strength (Ref 17, 31, 32).

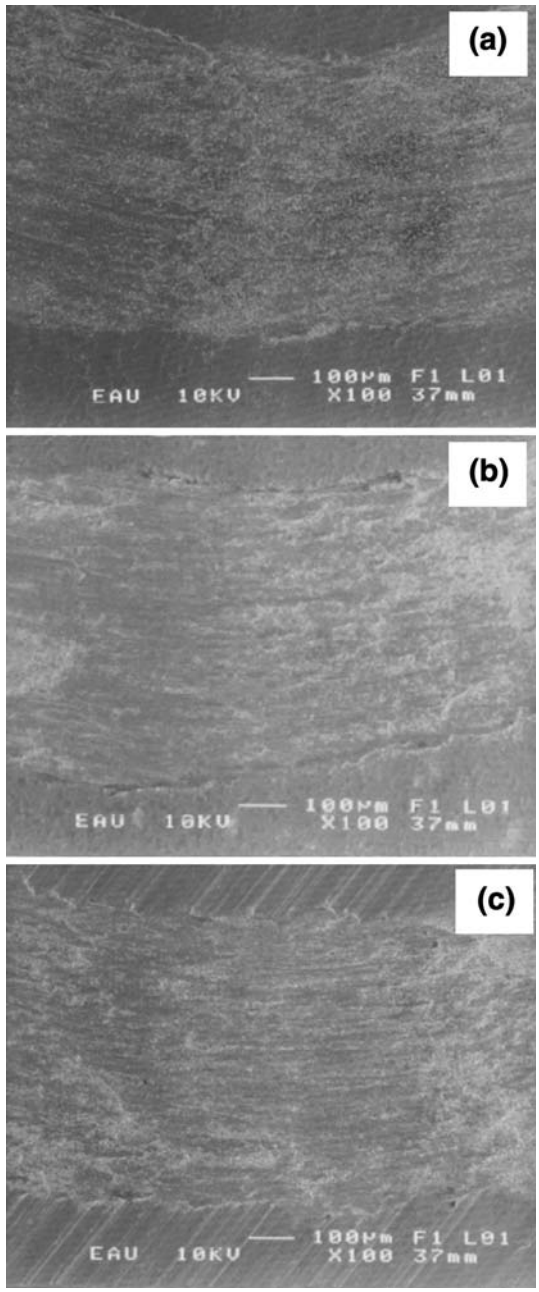

Fig. 7 The wear tracks of untreated CP-Ti: (a) Ra = 0.1 μm, (b) Ra = 0.3 μm, and (c) Ra = 0.6 μm

Figures 7 and 8 show the wear tracks of untreated and thermally oxidized CP-Ti with different surface roughness values. When the wear tracks of untreated CP-Ti were investigated, adhesive wear mechanisms were observed. In particular, the abrasive wear increased as roughness increased (Ref 33). The wear tracks had a wide and deep appearance. On the other hand, an abrasive wear mechanism was observed on the wear tracks of oxidized CP-Ti, due to the hard oxide layer (Ref 34). As shown in Fig. 8, flaking of the oxide layer was observed inside the wear tracks. Furthermore, the substrate roughness had an effect on the wear by fracture of oxide layer. As a result, abrasive and adhesive wear mechanisms occurred together. Track widths increased with the roughness, as seen in the untreated specimens.

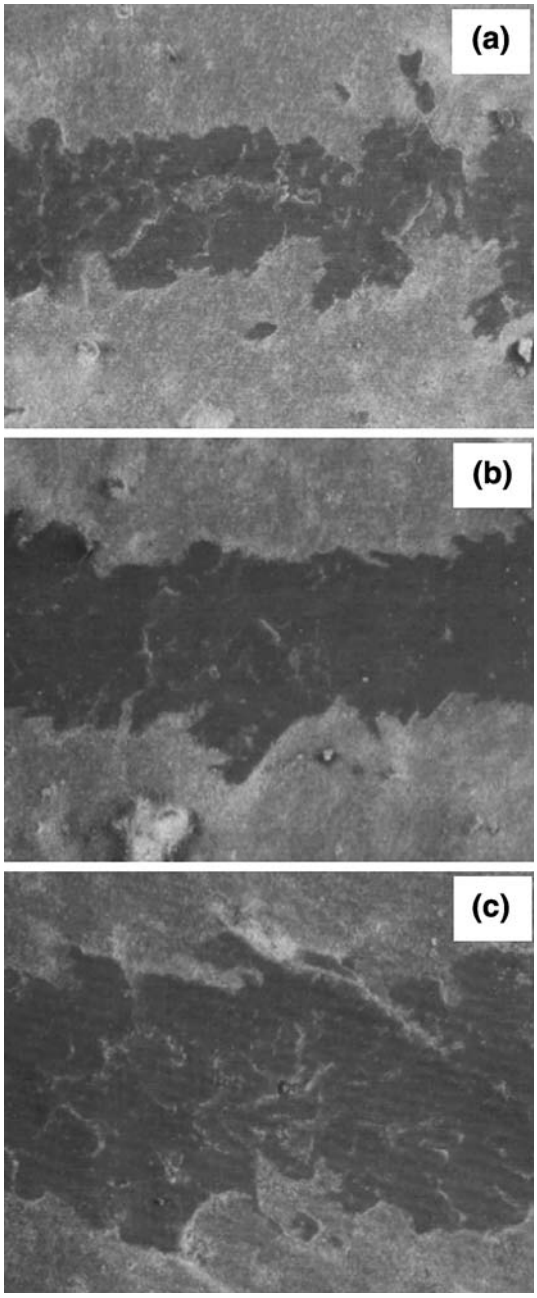

Fig. 8 The wear tracks of thermally oxidized CP-Ti: (a) *Ra* = 0.54 μm, (b) *Ra* = 0.64 μm, and (c) *Ra* = 0.7 μm

The anodic polarization curves of untreated and thermally oxidized CP-Ti in a 3% NaCl solution are shown in Fig. 9(a) and (b), respectively. It was observed that the E_{cor} (corrosion potential) and I_{cor} (corrosion current) values were affected by the surface roughness (Fig. 9). While the E_{cor} values of specimens with low roughness values increased, the I_{cor} values decreased. The corrosion potentials of the oxidized specimens were higher than that of the untreated specimens, while the corrosion potentials were comparable for each roughness value. The main cause of this increase is the thick and stable oxide layer formed after oxidation. The oxide layer formed on the surface of CP-Ti after thermal oxidation acts as a barrier and prevents the diffusion of Cl ions into the substrate material. In addition, the increase in the numbers of stable pits with

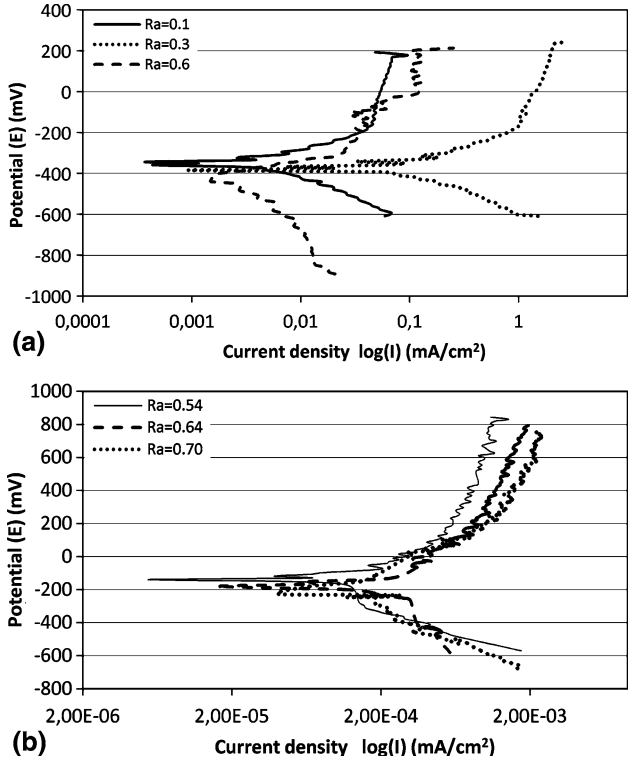

Fig. 9 The anodic polarization curves in a 3% NaCl solution: (a) untreated and (b) thermally oxidized CP-Ti

increasing surface roughness resulted in negative corrosion potential values for all samples (Ref 35, 36). As known, macrorough surfaces have a relatively higher ion release rate and lower corrosion resistance than microrough surfaces (Ref 20). The corrosion test results obtained in this study were consistent with the results given in the literature.

4. Conclusions

The effect of surface roughness on the mechanical, tribological, and corrosion properties of thermally oxidized CP-Ti was examined in this study. After thermal oxidation, it was observed that the surface roughness values increased. The single rutile phase was formed on the surface after oxidation. A diffusion zone in which the oxygen diffused under the oxide layer was observed. Furthermore, it was observed that the surface roughness had no effect on the preferred growth orientation of the rutile phase. While unstable and high friction coefficients were obtained with increasing roughness for untreated CP-Ti, this did not occur for the oxidized specimens. Similar results were also observed for the corrosion behaviors. As the surface roughness values decrease, the corrosion potentials shifted to higher values.

Acknowledgments

This research has been supported by TUBITAK (The Scientific and Technical Research Council of Turkey) project with Grant No. 107M313. The authors would like to thank the TUBITAK for funding the project.

References

1. D. Eylon and S.R. Seagle, Advances in Titanium Technology—An Overview, *Keikinzoku/J. Jpn. Inst. Light Metals*, 2000, **50**(8), p 359–370
2. W.L. Williams, *Proceedings of International Conference on Titanium: The Science, Technology and Application of Titanium*, Pergamon Press, London, 1970
3. J.R. Sobiecki, T. Wierzchon, and J. Rudnicki, The Influence of Glow Discharge Nitriding, Oxynitriding and Carbonitriding on Surface Modification of Ti-1Al-1Mn Titanium Alloy, *Vacuum*, 2001, **64**, p 41–46
4. F. Galliano, E. Galvanetto, S. Mischler, and D. Landolt, Tribocorrosion Behavior of Plasma Nitrided Ti-6Al-4 V Alloy in Neutral NaCl Solution, *Surf. Coat.Technol.*, 2001, **145**, p 121–131
5. H. Shibata, K. Tokaji, T. Ogava, and C. Hori, The Effect of Gas Nitriding on Fatigue Behaviour in Titanium Alloys, *Int. J. Fatigue*, 1994, **16**, p 370–376
6. A. Grill and P.R. Aron, RF-Sputtered Silicon and Hafnium Nitride—Properties and Adhesion to 440C Stainless Steel, NASA Technical Paper, 1983
7. S. Malinov, Z. Guo, W. Sha, and A. Wilson, Differential Scanning Calorimetry Study and Computer Modeling of $\beta \Rightarrow \alpha$ Phase Transformation in a Ti-6Al-4V Alloy, *Metall. Mater. Trans. A*, 2001, **32**, p 879–887
8. K.T. Rie, T. Stucky, R.A. Silva, and E. Leitao, Plasma Surface Treatment and PACVD on Ti Alloys for Surgical Implants, *Surf. Coat. Technol.*, 1995, **74–75**, p 973–980
9. T. Bell, J. Lanagan, P.H. Morton, H.W. Bergmann, and A.M. Staines, Surface Engineering of Titanium with Nitrogen, *Surf. Eng.*, 1986, **2**, p 133–143
10. S.K. Wu, H.C. Lin, and C.Y. Lee, Gas Nitriding of an Equiatomic TiNi Shape Memory Alloy: II. Hardness, Wear and Shape Memory Ability, *Surf. Coat. Technol.*, 1999, **113**(1–2), p 13–16
11. K.G. Budinski, Tribological Properties of Titanium Alloys, *Wear*, 1991, **151**, p 203–217
12. P.D. Miller and J.W. Holladay, Friction and Wear Properties of Titanium, *Wear*, 1958, **2**, p 133–140
13. M. Khaled, B.S. Yilbas, and J. Shirokoff, Electrochemical Study of Laser Nitrided and PVD TiN Coated Ti-6Al-4 V Alloy: The Observation of Selective Dissolution, *Surf. Coat. Technol.*, 2001, **148**, p 46–54
14. A.S. Korhonen and E. Harju, Surface Engineering with Light Alloys-Hard Coatings, Thin Films, and Plasma Nitriding, *J. Mater. Eng. Perform.*, 2000, **9**, p 302–305
15. B.Y. Chou and E. Chang, Plasma-Sprayed Hydroxyapatite Coating on Titanium Alloy with ZrO_2 Second Phase and ZrO_2 Intermediate Layer, *Surf. Coat. Technol.*, 2002, **153**, p 84–92
16. S.M. Johns, T. Bell, M. Samandi, and G.A. Collins, Wear Resistance of Plasma Immersion Ion Implanted Ti6A14V, *Surf. Coat. Technol.*, 1996, **85**, p 7–14
17. A. Bloyce, P.Y. Qi, H. Dong, and T. Bell, Surface Modification of Titanium Alloys for Combined Improvements in Corrosion and Wear Resistance, *Surf. Coat. Technol.*, 1998, **107**(2–3), p 125–132
18. C.Q. Yuan, Z. Peng, X.P. Yan, and X.C. Zhou, Surface Roughness Evolutions in Sliding Wear Process, *Wear*, 2008, **265**(3–4), p 341–348
19. B.J. Roylance, Wear Debris and Associated Wear Phenomena-Fundamental Research and Practice, *Proc. Inst. Mech. Eng. J: J. Eng. Tribol.*, 2000, **214**, p 79–105
20. G. Chen, X. Wen, and N. Zhang, Corrosion Resistance and Ion Dissolution of Titanium with Different Surface Microroughness, *Bio-Med. Mater. Eng.*, 1998, **8**, p 61–74
21. G. Bertrand, K. Jarraya, and J.M. Chaix, Morphology of Oxide Scales Formed on Titanium, *Oxid. Met.*, 1983, **21**(1–2), p 1–19
22. H. Dong, A. Bloyce, P.H. Morton, and T. Bell, Surface Engineering to Improve Tribological Performance of Ti-6Al-4V, *Surf. Eng.*, 1997, **135**, p 402–406
23. T. Bacci, F. Borgioli, E. Galvanetto, F. Galliano, and B. Tesi, Wear Resistance of Ti-6Al-4V Alloy Treated by Means of Glow-Discharge and Furnace Treatments, *Wear*, 2000, **240**, p 199–206
24. Z.X. Zhang, H. Dong, T. Bell, and B. Xu, The Effect of Treatment Condition on Boost Diffusion of Thermally Oxidised Titanium Alloy, *J. Alloys Compd.*, 2007, **431**(1–2), p 93–99
25. F. Habashi, *Handbook of Extractive Metallurgy*, Wiley-VCH, Weinheim, 1989, p 1130–1179
26. P.A. Dearnley, K.L. Dahm, and H. Cimenoglu, The Corrosion-Wear Behaviour of Thermally Oxidised Cp-Ti and Ti-6Al-4V, *Wear*, 2004, **256**(5), p 469–479
27. H. Dong and T. Bell, Enhanced Wear Resistance of Titanium Surfaces by a New Thermal Oxidation Treatment, *Wear*, 2000, **238**(2), p 131–137
28. H. Dong and X.Y. Li, Oxygen Boost Diffusion for the Deep-Case Hardening of Titanium Alloys, *Mater. Sci. Eng. A*, 2000, **280**(2), p 303–310
29. W. Yan and X.X. Wang, Surface Hardening of Titanium by Thermal Oxidation, *J. Mater. Sci.*, 2004, **39**, p 5583–5585
30. D. Siva Rama Krishna, Y.L. Brama, and Y. Sun, Thick Rutile Layer on Titanium for Tribological Applications, *Tribol. Int.*, 2007, **40**(2), p 329–334
31. D. Maugis, G. Desalos-Andarell, A. Heurtal, and R. Courtal, Adhesion and Friction on Al Thin Foils Related to Observed Dislocation Density, *ASLE Trans.*, 1978, **21**, p 1–19
32. M.N. Gardos, H.S. Hong, and W.O. Winer, Effect of Anion Vacancies on the Tribological Properties of Rutile (TiO_{2-x}). Part II. Experimental Evidence, *Tribol. Trans.*, 1990, **22**, p 209–222
33. P.J. Blau, C.B. Jolly, J. Qu, W.H. Peter, and C.A. Blue, Tribological Investigation of Titanium-Based Materials for Brakes, *Wear*, 2007, **263**(7–12), p 1202–1211
34. R.S. Magaziner, V.K. Jain, and S. Mall, Wear Characterization of Ti-6Al-4V Under Fretting-Reciprocating Sliding Conditions, *Wear*, 2008, **264**(11–12), p 1002–1014
35. T. Hong and M. Nagumo, Effect of Surface Roughness on Early Stages of Pitting Corrosion of Type 301 Stainless Steel, *Corros. Sci.*, 1997, **39**, p 1665–1672
36. R. Narayanan and S.K. Seshadri, Point Defect Model and Corrosion of Anodic Oxide Coatings on Ti-6Al-4V, *Corros. Sci.*, 2008, **50**, p 1521–1529